# Measuring complexity in a business cycle model of the Kaldor-type

*Dedicated to the Memory of Professor J. Sousa Ramos*

Cristina Januário[1], Clara Grácio[2] and Jorge Duarte[3]

[1,3] *ISEL-High Institute of Engineering of Lisbon, Department of Chemistry, Mathematics Unit,*
*Rua Conselheiro Emídio Navarro, 1949-014 Lisboa, Portugal*
*E-mail: cjanuario@deq.isel.ipl.pt*
*E-mail: jduarte@deq.isel.ipl.pt*
[2] *Department of Mathematics, Universidade de Évora, Rua Romão Ramalho, 59, 7000-585 Évora, Portugal*
*E-mail: mgracio@uevora.pt*

**Abstract**

The purpose of this paper is to study the dynamical behavior of a family of two-dimensional nonlinear maps associated to an economic model. Our objective is to measure the complexity of the system using techniques of symbolic dynamics in order to compute the topological entropy. The analysis of the variation of this important topological invariant with the parameters of the system, allows us to distinguish different chaotic scenarios. Finally, we use a another topological invariant to distinguish isentropic dynamics and we exhibit numerical results about maps with the same topological entropy. This work provides an illustration of how our understanding of higher dimensional economic models can be enhanced by the theory of dynamical systems.

*Key words:* Kaldor model, triangular maps, topological entropy, chaos.

## Introduction

The application of dynamical systems to economics is an enormous and interesting area, but it is a subject that is not systematically studied. In fact, the theory of dynamical systems (via differential equations and discrete time maps) has only been applied, in a large scale, to economic analysis in recent

years. One of the most interesting theories of business cycles in the Keynesian vein is still the work of Nicholas Kaldor [12]. The main difference from most other contemporary models consists in the use of non-linear functions, which produce endogenous cycles, rather than the linear multiplier-accelerator model which maintain regular cycles due to exogenous factors. The mathematical models that describe and mimic the behavior of economies appear from the relationships between different variables, such as, employment, income or savings. In Kaldor's model, investment and savings depend on the economic activity in a nonlinear relationship, although the usual formulation of the Kaldor model restricts the nonlinear relationship to the investment relation, with a linear relation for savings. Chang and Smyth [3] translated Kaldor's trade cycle model into a more rigorous context: the former into a limit cycle and the latter into catastrophe theory. One of the factors that difficult the mathematical treatment of the economic models, in general, is that they are, in the majority of the cases, described by models of dimension greater than one. There are few generalizations that can be made about high-dimensional dynamics from low-dimensional dynamics. The possibility of measuring significant quantities becomes very difficult. Therefore, a geometrical understanding of how these systems behave is, in general and from an intuitive standpoint, very insightful. In the present paper we consider the discrete two-dimension economic model of the Kaldor type, due to Hermann [10] and studied by many authors. For additional literature about different studies concerning the Kaldor model, the reader is also referred to [4], [5] [6], [11], [14] and [18].
In the present work, we will focus our attention on the study of a particular case of the chosen Kaldor model version. We provide a contribution for its detailed analysis, more precisely, using techniques of symbolic dynamics, we compute the topological entropy and we study some important features of its dynamics. We show the influence of the different parameters of the system on the variation of the topological entropy. This measure quantifies the amount of chaos in the dynamical system and allows us to distinguish different states of complexity. We also introduce a second invariant to distinguish maps with the same topological entropy and, in particular, how this second invariant changes within a given type of topological entropy level set (see some applications in other context in [8] and [7]). As far as the concept of entropy is concerned, it was originally developed in a branch of physics - the thermodynamics - and it has been adapted and applied in other different research areas such as: thermoeconomics, information theory, evolution and string theory. As an example, we can mention the work developed in [9], where a number of interconnected issues involving superstring theory, entropy and the particle content of the standard model of high energy physics, have been studied.

The Kaldor business cycle model consists in two principal equations using the following four variables: investments, capital stock, savings and income. Let us denote investments by $I$, capital stock by $K$, savings by $S$ and income by

$Y$. So, we have:

$$\begin{cases} Y_{t+1} - Y_t = \alpha(I_t - S_t) \\ K_{t+1} = (1-\delta)K_t + I_t \end{cases}, \tag{1}$$

where $\alpha$ is a positive number and represents the speed of reaction to the excess demand and $\delta$ $(0 < \delta < 1)$ represents the capital stock depreciation rate. A value of $\alpha$ smaller than one means a prudent reaction. Conversely, a high value of $\alpha$ means rash reactions. The state of an economy modeled by this discrete version of the Kaldor model is completely determined by the income and the capital stock.
Savings are such that,

$$S_t = Y_t - C(Y_t), \tag{2}$$

where $C(Y_t)$, the consumption function, has a sigmoid shape similar to Kaldor's investment function:

$$C(Y_t) = c_0 + \frac{20}{\pi} \arctan\left(\frac{c\pi(Y_t - Y^*)}{20}\right), \tag{3}$$

with $c_0$, $c$ and $Y^*$ constants. The parameters $c_0$ and $c$ are related with the sigmoidal shape of the consumption function. $Y^*$ represents the equilibrium level of income. Net investment depends proportionally on possible discrepancies

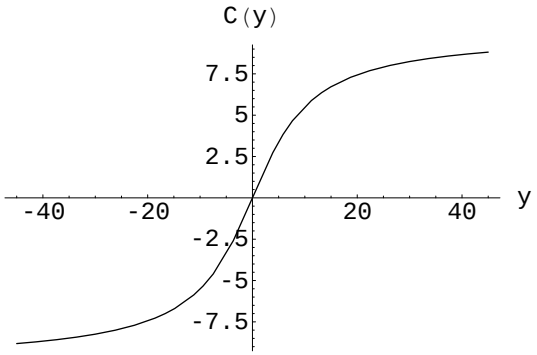


Fig. 1. The shape of the consumption function, $C(Y_t)$, for $c_0 = 0$ and $Y^* = 0$.

between the desired capital stock, $K_t^d$, and actual capital stock:

$$I_t = \beta(K_t^d - K_t) + \delta K_t. \tag{4}$$

Considering the desired capital stock depending linearly on income,

$$K_t^d = \gamma Y_t,$$

and inserting expressions (2) and (4) in equation (1) we have the following two dimensional nonlinear map:

$$\begin{cases} Y_{t+1} = \alpha(\beta\,(\gamma Y_t - K_t) + \delta K_t + C(Y_t) - Y_t) + Y_t \\ K_{t+1} = (1-\beta)K_t + \beta\ \gamma Y_t \end{cases}, \tag{5}$$

where the system parameters satisfy: $\alpha, c, \gamma > 0$, $0 < \delta, \beta < 1$ and $C(Y_t)$ is given by Eq. 3.

Considering the particular case, when $\beta = \delta$, the map becomes:

$$\begin{cases} Y_{t+1} = \alpha\left(\beta\gamma Y_t + c_0 + \frac{20}{\pi}\arctan\left(\frac{c\pi(Y_t - Y^*)}{20}\right) - Y_t\right) + Y_t \\ K_{t+1} = (1-\beta)K_t + \beta\ \gamma Y_t \end{cases}. \tag{6}$$

This map have the peculiarity that its first component doesn't depend on the second, and it is called a triangular map (or skew map). An immediate consequence of this structure is that the first equation works like an independent one-dimensional map, which means, from the economic point of view, that the income depends only on the income itself. The first component of the map is called the *basis map* and the second is called the *fiber map*. A second consequence of this triangular structure is the possibility to apply mathematical methods to compute relevant quantities that characterize the system as chaotic or non chaotic.
The outline of the paper is as follows. In Section 1 we present the model and investigate its dynamics. In Section 2 we introduce the symbolic dynamics techniques necessary to our study of the model and the main results related to the computation of topological entropy. We illustrate the computation of this numerical invariant and we show its variation with the different relevant parameters of the system. In Section 3 we study the second topological invariant in a specific entropy level set and, finally, in the last section we make some final considerations.

## 1 Triangular maps and chaos

Consider the family $F : \mathbb{R}^2 \longrightarrow \mathbb{R}^2$, $F(y,k) = (f(y), g(y,k))$ given by

$$F\begin{pmatrix} y \\ k \end{pmatrix} = \begin{pmatrix} \alpha\left(\beta\gamma\ y + c_0 + \frac{20}{\pi}\arctan\left(\frac{c\pi\ (y-y^*)}{20}\right) - y\right) + y \\ (1-\beta)k + \beta\ \gamma y \end{pmatrix} \tag{7}$$

where $\alpha, \delta, \gamma$ and $\beta$ are real parameters such that $\alpha, \delta, \gamma > 0$, $0 < \beta < 1$. The Fig. 2 and the Fig. 3 show the graphical representation of attractors associated to $F$ for some values of the parameters.

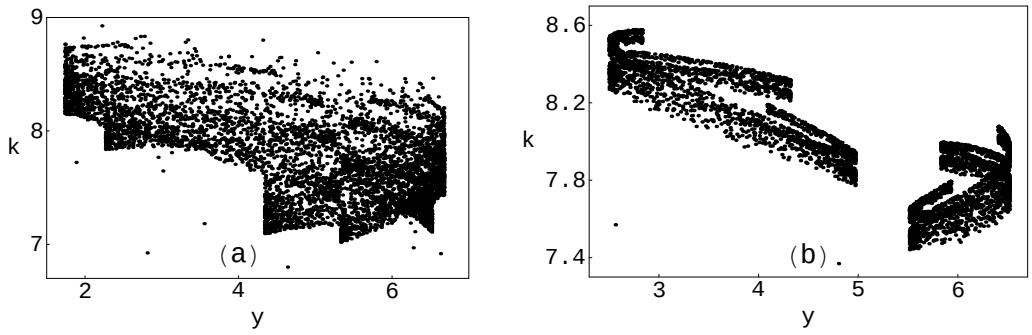


Fig. 2. Attractors associated to the family $F$ for some values of the parameters. In plot $(a)$ $\alpha = 20.3$, $\beta = 0.2$, $c = 0.75$, $\gamma = 1.65$ and in plot $(b)$ $\alpha = 21.5$, $\beta = 0.2$, $c = 0.75$, $\gamma = 1.65$.

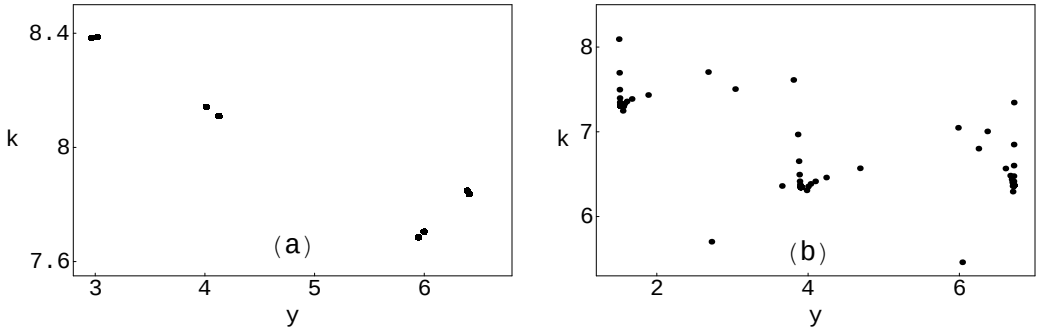


Fig. 3. Attractors associated to the family $F$ for some values of the parameters. In plot $(a)$ $\alpha = 19.5$, $\beta = 0.2$, $c = 0.75$, $\gamma = 1.65$ and in plot $(b)$ $\alpha = 21.84$, $\beta = 0.2$, $c = 0.75$, $\gamma = 1.65$.

Let $P = \{x_0,\ x_1,\ ...,\ x_{p-1}\}$ be a periodic orbit of period $p$ of the map $f$ such that $f(x_i) = x_{i+1}$ for $i = 0, ..., p-2$ and $f(x_{p-1}) = x_0$. We define the map $g_p : Y \longrightarrow Y$ as

$$g_p(y) = g(x_{p-1},\ g(x_{p-2}, ...g(x_1,\ g(x_0,\ y))...)). \tag{8}$$

If $Q = \{y_0,\ y_1,\ ...,\ y_{q-1}\}$ is a periodic orbit of period $q$ of the map $g_p$ such that $g_p(y_i) = y_{i+1}$ for $i = 0, ..., q-2$ and $g_p(y_{p-1}) = y_0$, we can define the product $P.Q$ as the set containing the $p.q$ pairs:

$$\begin{array}{cccc}
(x_0, y_0) & (x_1, g(x_0, y_0)) & \dots & (x_{p-1}, g(x_{p-2}, ...g(x_1, g(x_0, y_0))...)) \\
(x_0, y_1) & (x_1, g(x_0, y_1)) & \dots & (x_{p-1}, g(x_{p-2}, ...g(x_1, g(x_0, y_1))...)) \\
\vdots & \vdots & \ddots & \vdots \\
(x_0, y_{q-1}) & (x_1, g(x_0, y_{q-1})) & \dots & (x_{p-1}, g(x_{p-2}, ...g(x_1, g(x_0, y_{q-1}))...)).
\end{array}$$

The orbits of the one-dimensional maps $f$ and $g_p$ determine the orbits of the

triangular map $T$, as we show in the following Lemma:

**Lemma 1** *Let $T = (f, g) : X \times Y \longrightarrow X \times Y$ be a continuous triangular map. Then the following hold:*
*(1) If $f$ has a periodic orbit $P$ and $g_p$ has a periodic orbit $Q$, then $P.Q$ is a periodic orbit of $T$.*
*(2) Conversely, each periodic orbit of $T$ can be obtained as a product of a periodic orbit $P$ of $f$ by a periodic orbit of $g_p$.*

**PROOF.** See [2].

The topological entropy is a measure of complexity of a dynamical system. Let $T$ be a triangular map like defined in the earlier Lemma. The Bowen's formula for the inferior and superior values of the topological entropy of $T$, $h_{top}(T)$, is valid, that is,

$$\max\{h_{top}(f), h_{top}(g_p)\} \leq h_{top}(T) \leq h_{top}(f) + h_{top}(g_p), \tag{9}$$

where $h_{top}(f)$ and $h_{top}(g_p)$ represent, respectively, the topological entropy of the basis map, $f$, and the topological entropy of the fiber map associated to the orbit $P$, $g_p$.

According to (9), to compute topological entropy it is necessary to compute first the topological entropy of $f$, a 4-parameter family representing the basis map,

$$f(y) = \alpha\left(\beta\gamma\ y + c_0 + \frac{20}{\pi}\arctan\left(\frac{c\pi\ (y - y^*)}{20}\right) - y\right) + y \tag{10}$$

Observing the solutions of the equation $f'(y) = 0$ we can see that the map $f$ is a bimodal map, that is, a continuous map on the interval with three monotonic subintervals and two turning points $c_1$ and $c_2$ (see Figure 4), when $c > 1 - \beta\gamma - \frac{1}{\alpha} > 0$. This is the situation we will consider. The relative minimum $c_1$ and the relative maximum $c_2$ are given by:

$$c_1 = y^* - \sqrt{\frac{\frac{20^2 c}{1-\frac{1}{\alpha}-\beta\gamma} - 20^2}{c^2\pi^2}} \quad \text{and} \quad c_2 = y^* + \sqrt{\frac{\frac{20^2 c}{1-\frac{1}{\alpha}-\beta\gamma} - 20^2}{c^2\pi^2}}.$$

In order to study clearly the variation of the topological entropy of our family of maps, it is relevant to analyze the following cases:

*(1)* $c_0 = Y^* = 0$
*(2)* $c_0 \neq 0$ and $Y^* \neq 0$

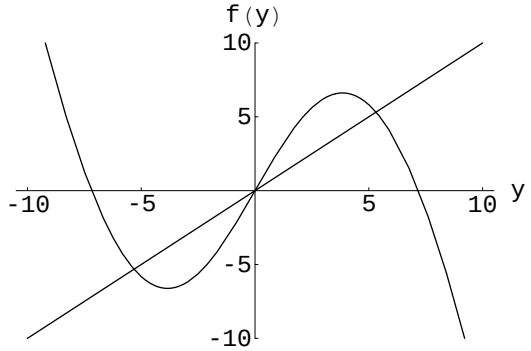


Fig. 4. Graphical representation of $f$ when $c > 1 - \beta\gamma - \frac{1}{\alpha}$. In this case $\alpha = 26.0$, $\beta = 0.2$, $c = 0.75$ and $\gamma = 1.65$.

Firstly, we are going to consider $c_0 = Y^* = 0$. In this case the turning points $c_1$ and $c_2$ are symmetric.

The figures Fig. 5 show the variation of the behavior of the basis map when we change one parameter, $\alpha$ or $c$, at the time. The other parameters, $\beta$ and $\gamma$, modify the bimodal map in the same way as the parameter $c$.

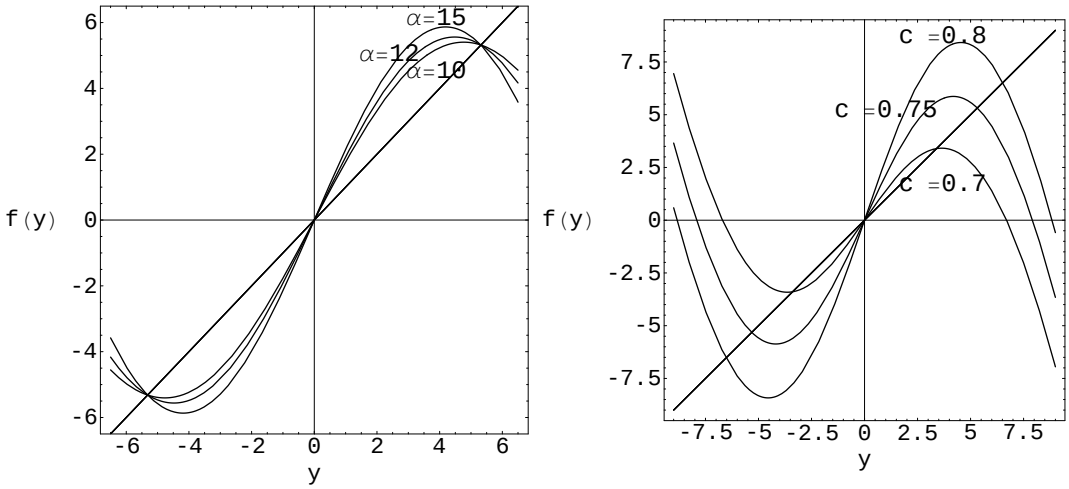


Fig. 5. The behavior of the basis map. In plot $a$) when $\alpha$ varies, the other parameters are: $\beta = 0.2$, $c = 0.75$ and $\gamma = 1.65$. In plot $b$) when $c$ varies, the other parameters are: $\alpha = 15$, $\beta = 0.2$ and $\gamma = 1.65$.

We are now in position to exhibit some interesting properties of the topological entropy of the basis map for some value of the parameters.

Using techniques of symbolic dynamics, in particular some results concerning to Markov partitions associated to bimodal maps, we compute the topological entropy of the basis map for $c_0 = Y^* = 0$ (for more details see [13] and [16]). As we pointed out before, our basis map is a bimodal map. Therefore, the symbolic dynamics for cubic maps is particularly important to study our type of systems.

Let us consider a bimodal map $f$ (piecewise monotone map) on the interval $I = [c_0, c_3]$, where $I$ is subdivided into three subintervals:

$$L = [c_0, c_1[\,, \qquad M = ]c_1, c_2[\,, \qquad R = ]c_2, c_3]$$

such that, $f$ is strictly decreasing in $L$ and $R$ intervals, increasing in the interval $M$ and $c_1$ and $c_2$ denote, respectively, the relative minimum and the relative maximum of $f$. The points $c_1$ and $c_2$ play an important role. The dynamics of the interval is characterized by the symbolic sequences associated to the orbits of points $c_1$ and $c_2$. Such orbits are, respectively,

$$O(c_1) = \left\{x_i : x_i = f^i(c_1),\ i \in \mathbb{N}\right\} \quad \text{and} \quad O(c_2) = \left\{y_i : y_i = f^i(c_2),\ i \in \mathbb{N}\right\}.$$

We associate to each orbit $O(c_i)$ a sequence of symbols $S = S_1 S_2 ... S_j ... \in \Sigma = \{L, A, M, B, R\}^{\mathbb{N}}$, where

$$\begin{cases} S_j = L & \text{if } f^j(c_i) < c_1 \\ S_j = A & \text{if } f^j(c_i) = c_1 \\ S_j = M & \text{if } c_1 < f^j(c_i) < c_2 \\ S_j = B & \text{if } f^j(c_i) = c_2 \\ S_j = R & \text{if } f^j(c_i) > c_2 \end{cases}.$$

The set of symbols $\Sigma$ has an order relation that depends on the $LR$-parity. If we denote by $n_{LR}$ the number of times the symbols $L$ and $R$ occur in $S$ it is possible to define the $LR$-parity of a sequence, $\rho(S) = (-1)^{n_{LR}}$, meaning odd or even according to $n_{LR}$. Given $P$, $Q$ two sequences such that $P_1 P_2 ... P_{k-1} = Q_1 Q_2 ... Q_{k-1}$ and $P_k \neq Q_k$, if the $LR$-parity of the common block is even (that is, $\rho(P_1 P_2 ... P_{k-1}) = +1$) then $P < Q$ if $P_k < Q_k$ in the order $L < A < M < B < R$ and if the $LR$-parity of the common block is odd (that is, $\rho(P_1 P_2 ... P_{k-1}) = -1$) then $P < Q$ if $P_k < Q_k$ in the order $R < B < M < A < L$. If there is no such index $k$ then $P = Q$. When $O(c_1)$ or $O(c_2)$ is a $k$-periodic orbit the sequence of symbols can be characterized by a block of length $k$, $S^{(k)} = S_1 ... S_{k-1} C_i$. In what follows we restrict

our study to the case when $c_1$ and $c_2$ are periodic (respectively, eventually periodic) such that $O(c_1)$ is $p$-periodic and $O(c_2)$ is $q$-periodic (respectively, $f^p(c_1) = c_2$ or $f^q(c_2) = c_1$). We shall note that $O(c_1)$ is realizable iff the block $P = P_1...P_{p-1}A$ is maximal, that is, $\sigma^i(P) \leq P$, where $1 < i \leq p$ and $\sigma(P_iP_{i+1}P_{i+2}...) = P_{i+1}P_{i+2}...$ is the usual shift operator. Note also that $O(c_2)$ is realizable iff the block $Q = Q_1...Q_{q-1}B$ is minimal, that is, $\sigma^j(Q) \geq Q$, where $1 < j \leq q$. Finally, note that the pair of sequences that are realizable satisfies the following conditions $\sigma^i(P) \geq Q$, for $1 \leq i \leq p$ and $\sigma^j(Q) \leq P$, for $1 \leq j \leq q$. The set of such pair of sequences will be denoted by $\Sigma_{(A,B)}$. The pairs $\left(P^{(p)}, Q^{(q)}\right) \in \Sigma_{(A,B)}$ where $P^{(p)} = P_1...P_{p-1}A$, $Q^{(q)} = Q_1...Q_{q-1}B$, the bistable sequence $P_1...P_{p-1}BQ_1...Q_{q-1}A$, and the eventually periodic sequence $P_1...P_{p-1}BQ_1...Q_{q-1}B$ or.$Q_1...Q_{q-1}AP_1...P_{p-1}A$ are called kneading data.

In [16], Milnor-Thurston, introduced the concept of kneading increments and kneading-matrix. These are power series that measure the discontinuity evaluated at the turning points $c_i$, $i = 1, 2, ..., m$, of $m$-modal maps. For the case of bimodal maps we have two kneading-increments defined by

$$\nu_i(t) = \theta_{c_i^+}(t) - \theta_{c_i^-}(t),\ i = 1, 2$$

where $\theta_x(t)$ is the invariant coordinate of the sequence $S_0S_1S_2...S_j...$ associated to the itinerary of the point $x$. The invariant coordinate is defined by

$$\theta_x(t) = \sum_{j=0}^{\infty} \tau_j\ t^j\ S_j,$$

where $\tau_j = \prod_{i=0}^{J-1} \varepsilon(S_i)$ for $j > 0$, $\tau_0 = 1$ for $j = 0$,

$$\varepsilon(S_i) = \begin{cases} -1 \text{ if } S_i = L \\ 0 \text{ if } S_i = A \\ 1 \text{ if } S_i = M \\ 0 \text{ if } S_i = B \\ -1 \text{ if } S_i = R \end{cases}$$

and $\theta_{c_i^{\pm}}(t) = \lim_{x \to c_i^{\pm}} \theta_x(t)$. Separating the terms associated to the symbols $L$, $M$ and $R$, we obtain

$$\nu_i(t) = N_{i1}(t)\ L + N_{i2}(t)\ M + N_{i3}(t)\ R.$$

The $2 \times 3$ kneading-matrix is defined by

$$N(t) = \begin{bmatrix} N_{11}(t) & N_{12}(t) & N_{13}(t) \\ N_{21}(t) & N_{22}(t) & N_{23}(t) \end{bmatrix}$$

and the corresponding kneading determinent, $D(t)$, is

$$\begin{aligned} D(t) &= \frac{D_1(t)}{1-\varepsilon(L)t} = -\frac{D_2(t)}{1-\varepsilon(M)t} = \frac{D_3(t)}{1-\varepsilon(R)t} \\ &= \frac{D_1(t)}{1+t} = -\frac{D_2(t)}{1-t} = \frac{D_3(t)}{1+t}, \end{aligned}$$

where $D_1(t) = N_{12}(t)N_{23}(t) - N_{22}(t)N_{13}(t)$, $D_2(t) = N_{11}(t)N_{23}(t) - N_{21}(t)N_{13}(t)$ and $D_3(t) = N_{11}(t)N_{22}(t) - N_{21}(t)N_{12}(t)$.

Now we consider the topological entropy. As we pointed out before, this important numerical invariant is related to the orbit growth and allows us to quantify the complexity of the dynamics. It represents the exponential growth rate for the number of orbit segments distinguishable with arbitrarily fine but finite precision. In a sense, the topological entropy describes in a suggestive way the total exponential complexity of the orbit structure with a single number.

A definition of chaos in the context of one-dimensional dynamical systems states that a dynamical system is called chaotic if its topological entropy is positive. Thus, the topological entropy can be computed to express whether a map has chaotic behavior.

Let $s$ be the growth number of a bimodal map $f$. The topological entropy of $f$, denoted by $h_{top}(f)$, is given by

$$h_{top}(f) = \log s,$$

where

$$s = \frac{1}{t^*},$$

with $t^*$ the root of $D(t)$, which has the lowest modulus.

In order to illustrate the outlined formalism about the computation of the topological entropy, we discuss the following example.

**Example 2** *Let us fix* $\alpha = 21.054$, $\beta = 0.2$, $c = 0.75$ *and* $\gamma = 1.65$ *(see map of Figure 4). For this parameter values the orbits of the turning points define the pair of sequences* $(LMLLA, RMRRB)$. *The symbolic sequences that*

*correspond to the orbits of the points* $c_1^+$, $c_1^-$, $c_2^+$ *and* $c_2^-$ *are*

$$\begin{aligned} c_1^+ &\longrightarrow M\,(LMLLL)^\infty \\ c_1^- &\longrightarrow L\,(LMLLL)^\infty \\ c_2^+ &\longrightarrow R\,(RMRRR)^\infty \\ c_2^- &\longrightarrow M\,(RMRRR)^\infty . \end{aligned}$$

*Note that the block* $LMLLL$ *corresponds to the sequence* $LMLLA$ *where the symbol* $A$ *is replaced by* $L$ *because the parity of the block* $LMLL$ *is odd and the block* $RMRRR$ *corresponds to the sequence* $RMRRB$ *where the symbol* $B$ *is replaced by* $R$ *because the parity of the block* $RMRR$ *is odd. The invariant coordinates are*

$$\begin{aligned} \theta_{c_1^+}(t) &= M + Lt - Mt^2 - Lt^3 + Lt^4 - Lt^5 + Lt^6 - Mt^7 - ... \\ &= M + t\,(L - Mt - Lt^2 + Lt^3 - Lt^4) + t^6(L - Mt - Lt^2 + Lt^3 - Lt^4) + ... \\ &= M + t\,(L - Mt - Lt^2 + Lt^3 - Lt^4)\,(1 + t^5 + t^{10} + ...) \\ &= M + \tfrac{t\left(L - Mt - Lt^2 + Lt^3 - Lt^4\right)}{1 - t^5}, \\ \theta_{c_1^-}(t) &= L - Lt + Mt^2 + Lt^3 - Lt^4 + Lt^5 - Lt^6 + Mt^7 + ... \\ &= L - t\,(L - Mt - Lt^2 + Lt^3 - Lt^4) - t^6(L - Mt - Lt^2 + Lt^3 - Lt^4) - ... \\ &= L - t\,(L - Mt - Lt^2 + Lt^3 - Lt^4)\,(1 + t^5 + t^{10} + ...) \\ &= L - \tfrac{t\left(L - Mt - Lt^2 + Lt^3 - Lt^4\right)}{1 - t^5} \end{aligned}$$

*and*

$$\begin{aligned} \theta_{c_2^+}(t) &= R - Rt + Mt^2 + Rt^3 - Rt^4 + Rt^5 - Rt^6 + Mt^7 - ... \\ &= R - t\,(R - Mt - Rt^2 + Rt^3 - Rt^4) - t^6(R - Mt - Rt^2 + Rt^3 - Rt^4) - ... \\ &= R - t\,(R - Mt - Rt^2 + Rt^3 - Rt^4)\,(1 + t^5 + t^{10} + ...) \\ &= R - \tfrac{t\left(R - Mt - Rt^2 + Rt^3 - Rt^4\right)}{1 - t^5}, \\ \theta_{c_2^-}(t) &= M + Rt - Mt^2 - Rt^3 + Rt^4 - Rt^5 + Rt^6 - Mt^7 + ... \\ &= M + t\,(R - Mt - Rt^2 + Rt^3 - Rt^4) + t^6(R - Mt - Rt^2 + Rt^3 - Rt^4) - ... \\ &= M + t\,(R - Mt - Rt^2 + Rt^3 - Rt^4)\,(1 + t^5 + t^{10} + ...) \\ &= M + \tfrac{t\left(R - Mt - Rt^2 + Rt^3 - Rt^4\right)}{1 - t^5}. \end{aligned}$$

*The kneading increments, $\nu_1$ and $\nu_2$, are given by*

$$\begin{aligned}\nu_1(t) &= \theta_{c_1^+}(t) - \theta_{c_1^-}(t)\\ &= M + \tfrac{t\left(L-Mt-Lt^2+Lt^3-Lt^4\right)}{1-t^5} - \left(L - \tfrac{t\left(L-Mt-Lt^2+Lt^3-Lt^4\right)}{1-t^5}\right)\\ &= \left(\tfrac{-1+2t-2t^3+2t^4-t^5}{1-t^5}\right)\ L + \left(\tfrac{1-2t^2-t^5}{1-t^5}\right)\ M\end{aligned}$$

*and*

$$\begin{aligned}\nu_2(t) &= \theta_{c_2^+}(t) - \theta_{c_2^-}(t)\\ &= R - \tfrac{t\left(R-Mt-Rt^2+Rt^3-Rt^4\right)}{1-t^5} - \left(M - \tfrac{t\left(R-Mt-Rt^2+Rt^3-Rt^4\right)}{1-t^5}\right)\\ &= \left(\tfrac{-1+2t^2+t^5}{1-t^5}\right)\ M + \left(\tfrac{1-2t+2t^3-2t^4+t^5}{1-t^5}\right)\ R.\end{aligned}$$

*From the previous definitions, the kneading matrix is*

$$N(t) = \begin{bmatrix} \frac{-1+2t-2t^3+2t^4-t^5}{1-t^5} & \frac{1-2t^2-t^5}{1-t^5} & 0 \\ 0 & \frac{-1+2t^2+t^5}{1-t^5} & \frac{1-2t+2t^3-2t^4+t^5}{1-t^5} \end{bmatrix}.$$

*Since $D(t) = \frac{D_1(t)}{1+t} = -\frac{D_2(t)}{1-t} = \frac{D_3(t)}{1+t}$, we obtain*

$$D(t) = \frac{\left(1-2t^2-t^5\right)\left(1-2t+2t^3-2t^4+t^5\right)}{(1-t)\left(1-t^5\right)^2}.$$

*Therefore $t^* = 0.660992...$ and the topological entropy is given by*

$$h_{top}(f) = \log\left(\frac{1}{t^*}\right) = 0.414012....$$

To see the long term behavior for different values of the parameters, we plot, in Fig. 6 and Fig. 7 typical bifurcation diagrams starting from the initial conditions $c_1$ and $c_2$.

With these figures it is easier to understand Fig. 8 and Fig. 9 that present some numerical results of the variation of the topological entropy with each of the parameters $\alpha$ and $c$, in some regions of the parameter space. For these values of the parameters, these graphs suggest that the topological entropy $h_{top}$ is monotone increasing. This behavior is determined by the symbolic sequences ordering associated to the successive orbits of the two turning points and allows us to distinguish the return maps.

As far as basis map is concerned, it is important to notice that for the parameter values corresponding to a stable periodic orbit of the basis map $f(y)$, $g_p(k)$ is given by

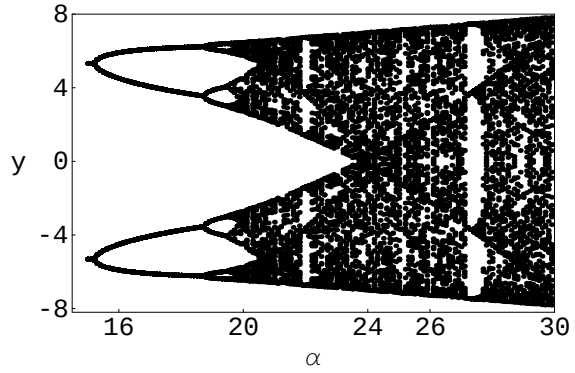


Fig. 6. Bifurcation diagram of the map $f$ for $\alpha \in [15, 30]$, $\beta = 0.2$, $c = 0.75$ and $\gamma = 1.65$.

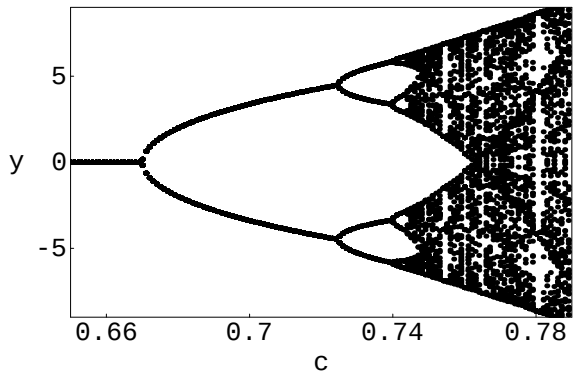


Fig. 7. Bifurcation diagram of the map $f$ for $c \in [0.63, 0.79]$, $\alpha = 21$, $\beta = 0.2$ and $\gamma = 1.65$.

$$\begin{aligned} g_p(k) &= g(y_{p-1}, \ldots g(y_2,\ g(y_1,\ g(y_0,\ k)) \ldots)) \\ &= (-1)^p k(-1+\beta)^p + \\ &\quad +\beta\left(y_{p-1} - y_{p-2}(-1+\beta) + y_{p-3}(-1+\beta)^2 - \ldots + (-1)^{p-1} y_0(-1+\beta)^{p-1}\right)\gamma. \end{aligned} \tag{11}$$

Note that $g_p(k)$ represents a straight line which means that the topological entropy is zero in the fiber map. In this situation we can enunciate that the topological entropy $h_{top}(F(y,k))$ of the map $F(y,k)$, representing the kaldor model considered, is such that

$$h_{top}(F(y,k)) = h_{top}(f(y)).$$

Concerning the study of the topological entropy, it may occur situations of isentropics dynamics (that is, dynamics with the same entropy) that can raise interesting questions.

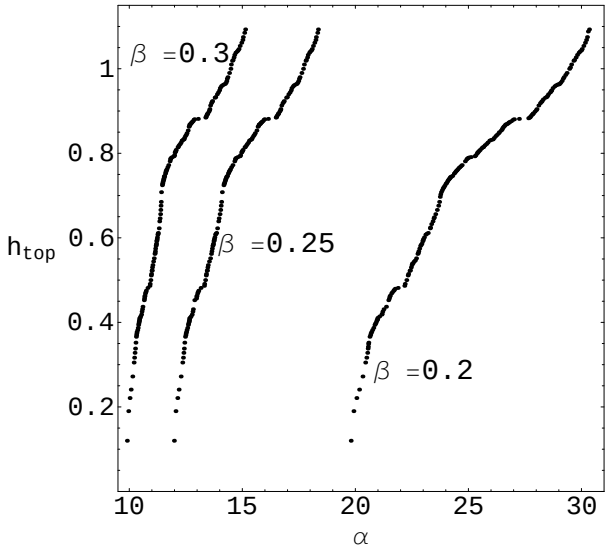


Fig. 8. Variation of the topological entropy with $\alpha$, for $c = 0.75$, $\gamma = 1.65$ and $\beta = 0.2$, $\beta = 0.25$ and $\beta = 0.3$.

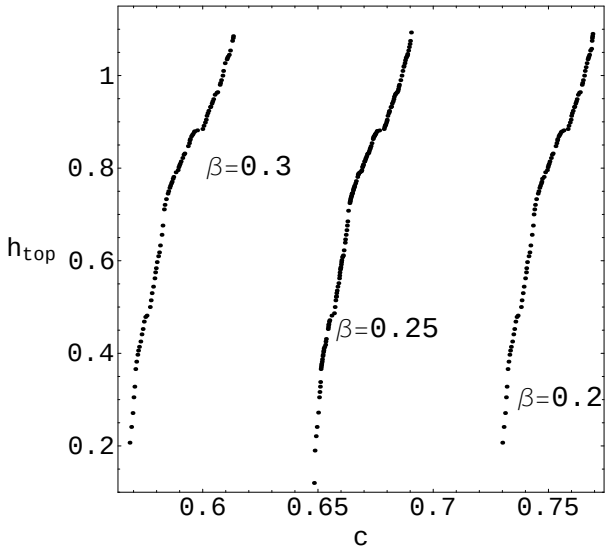


Fig. 9. Variation of the topological entropy with $c$,for $\alpha = 25.5$, $\gamma = 1.65$ and $\beta = 0.2$, $\beta = 0.25$ and $\beta = 0.3$.

## 2 Isentropic dynamics

To start with, let us consider the case pointed out before where

$$c_0 \neq 0 \quad \text{and} \quad Y^* \neq 0.$$

To illustrate this idea of isentropic dynamics, we are going to fix $Y^* = 0.8$, $\alpha = 22$, $\beta = 0.2$, $\gamma = 1.6$. and search for some maps with topological entropy $\log(2.147899...) = 0.764490...$, when parameters $c$ and $c_0$ change. In our study we consider the restriction of the family of maps

$$f_{c,c_o}(y) = \alpha \left( \beta\gamma \; y + c_0 + \frac{20}{\pi} \arctan\left( \frac{c\pi \; (y - y^*)}{20} \right) - y \right) + y$$

to its invariant region $\Omega \in \mathbb{R}^2$

$$\begin{aligned} \Omega = \{(c, c_0) \in \mathbb{R}^2 : f_{c,c_o}\left(f_{c,c_o}(c_1)\right) < f_{c,c_o}(c_2) \text{ and} \\ f_{c,c_o}\left(f_{c,c_o}(c_2)\right) > f_{c,c_o}(c_1) \text{ and } f_{c,c_o}(c_2) > c_2 \text{ and } f_{c,c_o}(c_1) < c_1\}, \end{aligned}$$

the set of parameters such that the basis map is bimodal.

The region $\Omega$ is presented in Fig.10.

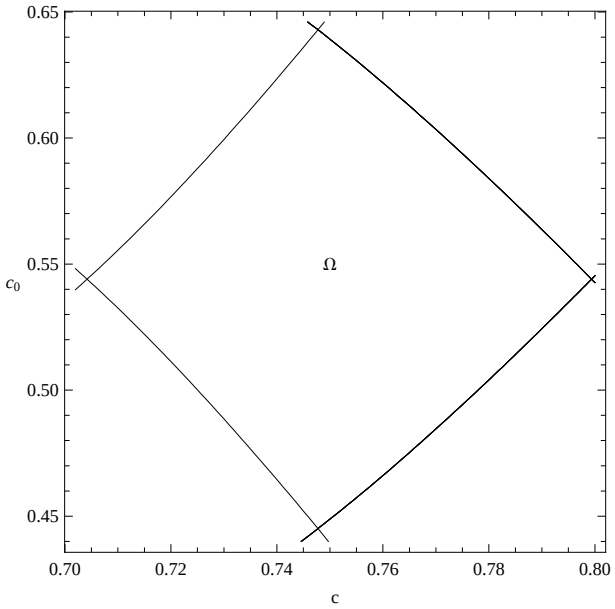


Fig. 10. The region $\Omega$ of the parameter space.

With the above procedure, we can compute the topological entropy for the maps. The following tables show the kneading data and the characteristic polynomial associated to each map. It is important to notice that the common factor $(-1 - 2t - t^2 + t^3)$ determines the spectral radius 2.147899.. and, there-

fore, the same topological entropy $h_{top}\left(f_{c,c_o}\right) = \log(2.147899...) = 0.764490...$,

| $(c, c_0)$ with $Y^* = 0.8$ | kneading data of $f_{c,c_o}$ |
|---|---|
| $(0.77505, 0.52026)$ | $(ALB, BRM^3A)$ |
| $(0.7729695, 0.528732)$ | $(ALMRB, BRM^3L^5MR^2MB)$ |
| $(0.77092, 0.54465)$ | $(ALM^2R^3B, BRM^2L^3M^2R^4MB)$ |
| $(0.775037, 0.567662)$ | $(ALM^3B, BRA)$ |
| $(0.772511, 0.557187)$ | $(ALM^3RB, BRML^5M^3R^2MB)$ |
| $(0.770934, 0.543232)$ | $(ALM^2RB, BRM^2L^5M^2R^2MB)$ |
| $(0.77295, 0.55914)$ | $(ALM^3R^3B, BRML^3M^3R^4MB)$ |
| $(0.7725154, 0.530723)$ | $(ALMR^3B, BRM^3L^3MR^4MB)$ |
| $(0.7743488, 0.523392)$ | $(ALMRM^3RB, BRM^3L^2M^3LM^2RM^3RMRMB)$ |
| $(0.771405, 0.5505)$ | $(ALM^2B, BRMA)$ |

| $(c, c_0)$ with $Y^* = 0.8$ | characteristic polynomial of $M(f_{c,c_o})$ |
|---|---|
| $(0.77505, 0.52026)$ | $(-1-2t-t^2+t^3)(-1+t-2t^2+t^3)$ |
| $(0.7729695, 0.528732)$ | $(-1-2t-t^2+t^3)(1-t)t^3$ $(-2+t-2t^2-t^4-t^5-t^6-t^7-t^9+t^{10})$ |
| $(0.77092, 0.54465)$ | $(-1-2t-t^2+t^3)(-1+t)t^6$ $(-2+t-2t^2-t^4-t^5-t^6-t^7-t^9+t^{10})$ |
| $(0.775037, 0.567662)$ | $(-1-2t-t^2+t^3)(-1+t)(1+t)$ $(-1+t-2t^2+t^3)$ |
| $(0.772511, 0.557187)$ | $(-1-2t-t^2+t^3)(-1+t)t^5$ $(-2+t-2t^2-t^4-t^5-t^6-t^7-t^9+t^{10})$ |
| $(0.770934, 0.543232)$ | $(-1-2t-t^2+t^3)(1-t)t^5$ $(-2+t-2t^2-t^4-t^5-t^6-t^7-t^9+t^{10})$ |
| $(0.77295, 0.55914)$ | $(-1-2t-t^2+t^3)(1-t)t^7$ $(-2+t-2t^2-t^4-t^5-t^6-t^7-t^9+t^{10})$ |
| $(0.7725154, 0.530723)$ | $(-1-2t-t^2+t^3)(1-t)t^5$ $(-2+t-2t^2-t^4-t^5-t^6-t^7-t^9+t^{10})$ |
| $(0.7743488, 0.523392)$ | $(-1-2t-t^2+t^3)t^7(-2+3t-t^2-2t^3+3t^4-4t^5$ $+4t^6-t^8+t^9-2t^{10}+t^{11}-t^{15}+t^{16}-2t^{17}+t^{18})$ |
| $(0.771405, 0.5505)$ | $(-1-2t-t^2+t^3)(-1+t-2t^2+t^3)$ |

At this point of our study, we emphasize that in all the examples we have chaotic behavior and the topological entropy has exactly the same value. One question appears naturally: how can we distinguish these isentropic maps?

In the following lines we address a contribution to the answer to this question.

It is interesting to exhibit a numerical result about the isentropic maps studied. To each point $(c_0, c)$ in Fig. 11 corresponds a map with the topological entropy $h_{top}(f_{c,c_o}) = \log(2.147899...) = 0.764490....$ We also represent the isentropic points in the $\Omega$ region (see Fig. 12).

The topological entropy by itself is no longer sufficient to classify the maps introduced. We need to consider a new topological invariant in order to distinguish the maps with the same entropy.

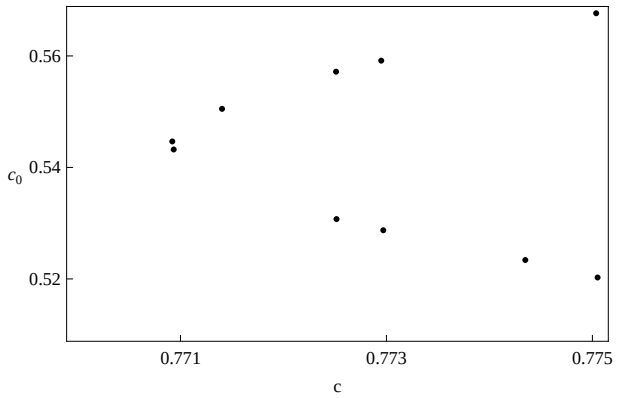


Fig. 11. Representation of points $(c, c_0)$, for $Y^* = 0.8$. To each point corresponds a map with topological entropy $h_{top}\left(f_{c,c_o}\right) = \log(2.147899...) = 0.764490....$

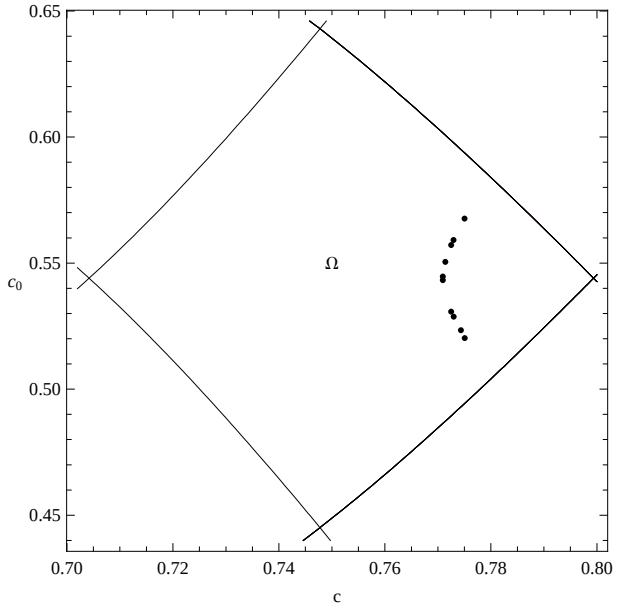


Fig. 12. Representation of points $(c, c_0)$, for $Y^* = 0.8$. To each point corresponds a map with topological entropy $h_{top}\left(f_{c,c_o}\right) = \log(2.147899...) = 0.764490....$

The study of topological classification for bimodal maps $f$ leads to the introduction of two topological invariants: one of them is the well known growth number $s\left(f\right) = e^{h_{top}(f)}$ and the other numerical quantity, denoted by $r$, is associated to the relative positions of the turning points of the map. The topological invariant $r$ is introduced using the hypothesis $s\left(f\right) > 1$ and the Milnor-Thurston results about the topologically semi-conjugate by $\lambda$ of $f_{c,c_0}$ to a piecewise linear map $F_{e,s}$ having slope $\pm s\left(f\right)$ everywhere (see [1], [16], [15] and [17]).

There exists one and only one map

$$F_{r,s} : [0,1] \longrightarrow [0,1] \qquad \text{so that} \qquad F_{r,s}\left(\lambda\left(x\right)\right) = \lambda\left(f_{c,c_0}\left(x\right)\right)$$

for every $x \in [0,1]$ such that

$$F_{r,s}\left(y\right) = \begin{cases} -s\ y + 1 & \text{if} \quad 0 \leq y < \lambda\left(c_1\right) \\ s\ y + r - 1 & \text{if} \quad \lambda\left(c_1\right) \leq y < \lambda\left(c_2\right) \\ -s\ y + s & \text{if} \quad y \geq \lambda\left(c_2\right) \end{cases}$$

where $\lambda\left(c_1\right) = (2-r)/(2s)$, $\lambda\left(c_2\right) = (1+s-r)/(2s)$ (see Fig. 13). Then, to

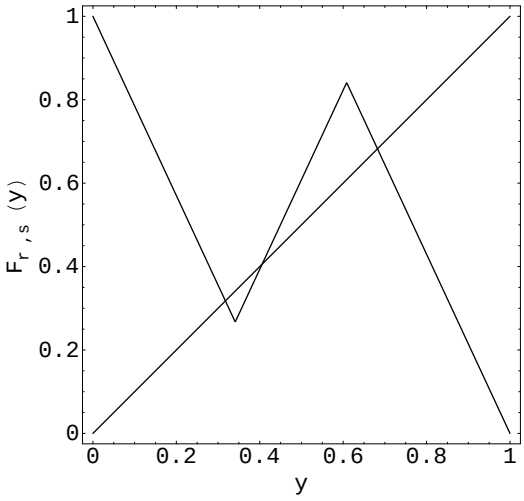


Fig. 13. Piecewise linear map for $s = 2.147899...$ and $r = 0.534428....$

each bimodal map $f_{c,c_0}$, characterized by a kneading sequence $(P^{(p)}, Q^{(q)})$, we can associate two topological invariants. One of them is the growth number $s\left(f\right)$, as we saw, and the other is the new invariant, $r(f)$, given by

$$r(f) = (3+e)/2 - s(\lambda\left(c_1\right) + \lambda\left(c_2\right))$$

with

$$\lambda\left(c_1\right) = \sum_{i=1}^{n_L+1} v_i \qquad \text{and} \qquad \lambda\left(c_2\right) = \sum_{i=1}^{n_L+n_M+2} v_i$$

where $n_L$ (resp. $n_M$) denote the number of symbols $L$ (resp. symbols $M$) and the vector $v$ is the Perron eigenvector associated to the eigenvalue $\lambda_{\max} = s$, $\mathcal{M}v = \lambda_{\max} v$, where $\mathcal{M}$ is the transition matrix with the extreme intervals $I_0 = [0, z_1]$ and $I_{p+q} = [z_{p+q}, 1]$ included. It is important to note that $r\left(f\right)$ is in fact a topological invariant because all the variables $\lambda\left(c_1\right)$, $\lambda\left(c_2\right)$ and $s\left(f\right)$ that lead to $r\left(f\right)$ are topological invariants (see [1]). In the piecewise linear case,

$F_{s,r}$, the parameter $r(f)$ is the invariant that distinguish isentropic dynamics and $r \in [0, 3-s]$.

Now regarding the previous considerations, we derive our main result

**Theorem 3** *The maps $f_{c,c_0}$ can be topologically classified by the pair of topological invariants $(s, r)$, where $s$ is the laps growth number $\left(s(f) = e^{h_{top}(f)}\right)$ and $r$ is the invariant given by*

$$r(f) = (3+e)/2 - s(\lambda(c_1) + \lambda(c_2)).$$

*and $\lambda$ the map defined by the semi-conjugacy to the piecewise linear map $F_{e,s}$.*

We discuss the following example which well illustrates the nature of our work.

**Example 4** *For the kneading data $(LMMMB, RA)$ we can apply the previous algorithm to compute the topological invariants associated to this sequence. The transition matrix*

$$\mathcal{M} = \begin{bmatrix} 0&0&0&1&1&1&1&1 \\ 0&1&1&0&0&0&0&0 \\ 0&1&1&1&0&0&0&0 \\ 0&0&0&0&1&0&0&0 \\ 0&0&0&0&0&1&0&0 \\ 0&0&0&0&0&0&1&0 \\ 0&0&1&1&1&1&1&0 \\ 1&1&0&0&0&0&0&0 \end{bmatrix}$$

*with $\mathcal{M}v = \lambda_{\max} v$ the equation of Perron eigenvector. Then we have*

$$\lambda(c_1) = \sum_{i=1}^{2} v_i = 0.341164... \quad \textit{and} \quad \lambda(c_2) = \sum_{i=1}^{6} v_i = 0.608378...$$

*(with $v$ normalized to the unit interval). We obtain*

$$s = 2.147899... \quad \textit{and} \quad r = 0.534428...$$

*The semi-conjugate piecewise linear map associated to this kneading data is given in the Fig. 13. The corresponding parameters of the map $f_{c,c_0}$ are $c = 0.775037$, $c_0 = 0.567662$ and $Y^* = 0.8$.*

To each kneading data $\left(P^{(p)}, Q^{(q)}\right)$ corresponds one and only one value of $r$.

For the set of points studied, we present in figures 14 and 15 some numerical results of the variation of the topological invariant $r$ with each of the param-

eters $c$ and $c_0$. The graphs of figures 12 and 14 have a similar shape which is a consequence of the relation between $r$ and $c_0$.

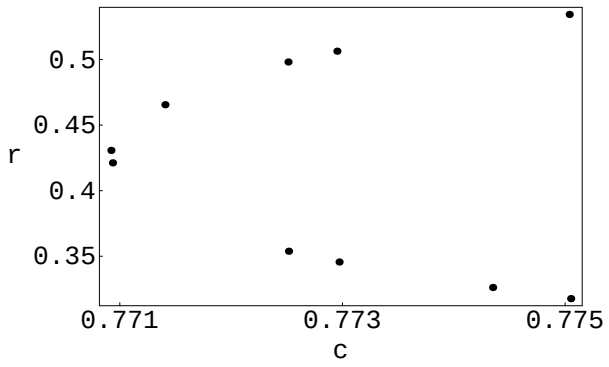


Fig. 14. Variation of the topological invariant $r$ with $c$.

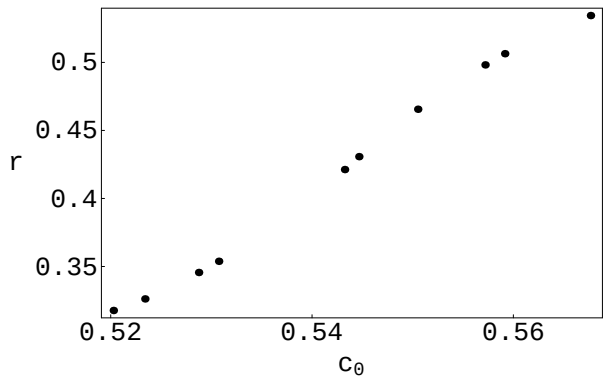


Fig. 15. Variation of the topological invariant $r$ with $c_0$.

Due to the fact that formula (11) is valid for all values of the parameters, the equality

$$h_{top}(F(y,k)) = h_{top}(f(y))$$

remains for $c_0 \neq 0$ and $Y^* \neq 0$. Therefore, the isentropic situations studied for $f(y)$ still occur for the triangular map $F(y,k)$.

## 3 Final considerations

In this article we have studied the chaotic dynamics of a Kaldor model, involving the income and the capital stock variables, in the case when it reduces to a map of the triangular type. In the available literature, the detailed examination of this model involves many different issues, both in the economic

and mathematical domains, and its scientific investigation is still an active research area.

A detailed analysis of the model became possible by the study of the variation of the topological entropy with the parameter $\alpha$ (that represents the speed of reaction to the excess demand) and with the parameter $c$ (which is directly related with the sigmoidal shape of the consumption function). Indeed, the Kaldor model exhibits positive topological entropy, which means that in certain conditions the associated economy has a chaotic nature. Our analysis reveals that when the parameter $\alpha$ increases (which means a rasher reaction to excess demand) the topological entropy also increases. In a similar way, when the parameter $c$ increases this numerical invariant also increases. Therefore, high values of these control parameters tend to introduce more complexity to the economy. To each value of these control parameters corresponds a value of the topological entropy which is a quantifier for the complex orbit structure and an atribute efficiently used to identify different chaotic states.

We introduced a second topological invariant as a tool to distinguish isentropic maps. It is interesting to notice that an increase in the control parameter $c_0$ means an increase in the numerical invariant $r$. Regarding our numerical simulations, is it possible to expect one identification of the parameter $c_0$ and the topological invariant $r$? In the context of economic models, what is the meaning of this topological invariant and what does it represent? These are open questions which may lead to future significant research works.

## References


[1] Almeida P, Lampreia JP, Sousa Ramos J. Topological invariants for bimodal maps. Iteration theory 1992; 1–8.

[2] Alsedà L, Llibre J. Periods for triangular maps. Bull. Austral. Math. Soc. 1993; 47: 41–53.

[3] Chang WW, Smith DJ. The existence and persistence of cycles in a non-linear model: Kaldor's 1940 model re-examined. Rev. Economic Studies 1971; 38: 37-44.

[4] Chu PC. First-passage time for stability analysis of the Kaldor model. Chaos Solitons & Fractals 2006; 27 (5): 1355-68.

[5] Dobrescu LI, Opris D. Neimark–Sacker bifurcation for the discrete-delay Kaldor model. Chaos Solitons & Fractals (2007), doi:10.1016/j.chaos.2007.10.044.

[6] Dohtani A, Misawa T, Inaba T, Yokoo M, Owase T. Chaos, complex transients and noise: illustration with a Kaldor model. Chaos Solitons & Fractals 1996; 7 (12): 2157-74.

[7] Duarte J, Silva L, Sousa Ramos J. The influence of coupling on chaotic maps modelling bursting cells. Chaos Solitons & Fractals 2006; 28: 1314-26.

[8] Duarte J, Sousa Ramos J. Topological invariants in forced piecewise-linear FitzHugh-Nagumo-like systems. Chaos Solitons & Fractals 2005; 23: 1553-65.

[9] EL Naschie, Superstrings, entropy and the elementary particles content of the standard model, *Chaos, Solitons & Fractals* 29, (2006), 48–54.

[10] Herrmann R. Stability and chaos in a Kaldor-type model. DP 22, Department of Economics, University of Goettingen; 1985.

[11] Januário C, Grácio C, Sousa Ramos J. Chaotic behavior in a two-dimensional business cycle model. ICDEA, Tenth International Conference on Difference Equations and Applications, Munich, Germany; 2005.

[12] Kaldor N. The Model of the Trade Cycle. Economic Journal 1940; 50: 78-92.

[13] Lampreia JP, Sousa Ramos J. Symbolic dynamics of bimodal maps. Portugal. Math. 1997; 54 (1): 1–18.

[14] Lorenz H-W. Nonlinear dynamical economics and chaotic motion. Springer, Berlin; 1993.

[15] Martins N, Severino R, Sousa Ramos J. Isentropic real cubic maps. Internat. J. Bifur. Chaos Appl. Sci. Engrg. 2003; 13 (7): 1701–09.

[16] Milnor J, Thurston W. On iterated maps of the interval I and II. Lect. Notes in Math 1988; 1342: 465-563.

[17] Ramos MM, Ramos CC, Severino R, Sousa Ramos J. Topological invariants of a chaotic pendulum. Int. J. Pure Appl. Math. 2004; 10 (2):209–26.

[18] Szydłowski M, Krawiec A. The stability problem in the Kaldor–Kalecki business cycle model. Chaos Solitons & Fractals 2005; 25 (2): 299-305.